THE MICROCIRCULATION: THEORY AND EXPERIMENT

Harvey N. Mayrovitz

A DISSERTATION

in

Bioengineering

Presented to the Faculty of the Graduate School of Arts and Sciences of the University of Pennsylvania in Partial Fulfillment of the Requirements for the Degree of Doctor of Philosophy.

1974

Abraham Noordergraaf
Supervisor of Dissertation

Lyle A. Peterson
Supervisor of Dissertation

Abraham Noordergraaf
Graduate Group Chairman

PART 1
CHAPTERS 1-2

ACKNOWLEDGEMENTS

Few, if any, scientific endeavors reach a successful and meaningful goal solely through the resources and efforts of one individual. As is known by those who have undertaken it, and as will be found by those embarking on it, the Doctoral Dissertation is no exception. From a technical point of view successful completion entails a research and scientific phase, as well as an often arduous phase of compiling and preparing the thesis document itself. But without the moral and financial support to carry on little technical accomplishment is possible. Through my academic activity and through each of the dissertation phases it has been my good fortune to have been the recipient of both advice and support of a caliber unsurpassed by any available. It is now my great honor to express publicly my sincere thanks to the following individuals.

To Dr. Abraham Noordergraaf, for his advice in the theoretical aspects of my research and thesis preparation, and for his continued support, guidance, and motivation throughout my academic and research activities. To Dr. Lysle H. Peterson for his advice in the physiological aspects of my research, his freely given personal interest, and continuing logistic and financial support. To Dr. Mary Wiedeman for her advice in the experimental and physiological aspects of my research, her warm personal interest and encouragement, and for providing animals and lab space to carry out much of the experimental work.

To Dr. Ernst Attinger for having provided me with my initial

exposure to cardiovascular research and for his financial support which allowed me to enter the field.

To Dr. Paul Hugenholtz for financial support which permitted me to carry out a portion of my research at the Thorax Center, Medical Faculty of Rotterdam as well as to obtain a rewarding educational experience abroad.

To Professor B. Th. Veltman for funding and logistics support which permitted me to carry out some of the theoretical work at Delft University.

To Mr. Decker for the use of the computer facilities at Delft University. To Mr. Zuidervart for useful technical discussions. To Simon Mëy and Curt van de Bent for their expert computer programming and data.

To Elmer Anderson for his expert drawings of many of the figures and untiring slide making.

To Melissa Manna for her critical and expert proofing and typing of much of the final manuscript.

To my children, Robert and Randall, for just being, and for showing an understanding well beyond their years of a father pursuing goals that they just now are coming to understand.

To my wife, Sandy, who through my academic training and research activities functioned not only as a mother, secretary and discussant but, in addition to her own professional activities, as a companion who shared the many problems I met along the way. And whose counsel often made the difference between carrying on and not.

To my mother, Rose, for her enduring encouragement.

To my father, Irving, whose calm, gentle, and well directed approach toward life provided me with an example, a goal, that I have yet to attain. It is to his loving memory that I dedicate this dissertation. Let it stand as a small tribute to his accomplishment.

This work was supported in part by Grant HL 10 330 08 and Program Project Research Grant HL 07762 from the U. S. P. H. S.

INDEX

TABLE OF CONTENTS

Appendix A... Variable Viscosity and Non-Newtonian Effects

Appendix B... Wall Equations

FIGURES

TABLES

BIBLIOGRAPHY

Attardi, G., and Attardi-Gandini, O.: Spontaneous peristaltic activity of veins of chick embryos and newly hatched chickens explanted in vitro, Experientia (Basel), 11:C7, 1955.

Attinger, E. O.: Wall properties of veins, I. E. E. Trans. Biomed. Eng., 16:253, 1969.

Attinger, E. O., and Anne, A.: Simulation of the cardiovascular system, Ann. N. Y. Acad. Sci., 128:810, 1966.

Attinger, E., Anne, A., Sugawara, H., and Mikami, T.: Analysis of pulsatile blood flow through a system of branched, nonuniform tubes, Proc. 4th Ann. Symp. Biomath., Memo #31, 1966.

Axelsson, J.: Dissociation of electrical and mechanical activity in smooth muscle, J. Physiol. (London), 158:381, 1962.

Baez, S.: Bayliss response in the microcirculation, Fed. Proc., 27:1410, 1968.

Baez, S.: Simultaneous measurements of radii and wall thickness of microvessels in the anesthetized rat, Circ. Res., 25:315, 1969.

Barnard, A. C., Lopez, L., and Hellums, J. D.: Basic theory of blood flow in capillaries, Microvas. Res., 1:1, 1969.

Barr, L., Berger, W., and Dewey, M. M.: Electrical transmission at the nexus between smooth muscle cells, J. Gen. Physiol., 51:347, 1968.

Bayliss, W. M.: The axial drift of the red cells when blood flows in narrow tubes, J. Physiol., 149:593, 1960.

Benekin, J. E., and de Witt, B.: A physical approach to hemodynamic aspects of the human cardiovascular system. In: Physical Basis of Circulatory Transport, Reeve, E. B., and Guyton, A. C., Eds. Philadelphia: W. B. Saunders Company, 1967. pp. 1-45.

Booz, K. H.: Experimental studies on the problem of the contractile activity of the portal vein in guinea pigs, Anat. Anz., 113:68, 1963.

Bugliarello, G., and Sevilla, J.: Velocity distribution and other characteristics of steady and pulsatile blood flow in fine glass tubes, Biorheology, 1:85, 1970.

Burch, G. E.: A Primer of Venous Pressure. Philadelphia: Lea and Febiger, 1950.

Burch, G. E., and Sodeman, W. A.: The estimation of the subcutaneous tissue pressure by a direct method, J. Clin. Invest., 16:845, 1937.

Charm, S., Kurland, G., and Brown, S. L.: The flow characteristics of blood suspensions, Biomedical Fl. Mech. Symp. Proc., pp. 89-93, 1967.

Chow, T. S., and Saibel, E.: Slow viscous flow of a shpere along a deformable tube, Biorheology, 6:307, 1970.

Christensen, R. M.: Viscoelastic properties of heterogeneous media, J. Mech. & Phys. of Solids, 17:23, 1969.

Copley, A. L.: Apparent viscosity and wall adherence of blood systems. In: Flow Properties of Blood, Copley, A. L., and Stainsby, G., Eds. London: Pergamon Press, 1960. pp. 97-117.

Cuthbert, A. W.: Electrical activity in mammalian veins, Bibl. Anat., 8:11, 1966.

D'Agrosa, L. S.: Patterns of venous vasomotion in the bat wing, Am. J. Physiol., 218:530, 1970.

Duling, B. R.: Microvascular responses to alterations in oxygen tension, Circ. Res., 31:481, 1972.

Duling, B. R., and Berne, R. M.: Microiontophoretic application of vasoactive agents to the microcirculation of the hamster cheek pouch, Microvas. Res., 1:158, 1968.

Duling, B. R., and Berne, R. M.: Longitudinal gradients in periarteriolar oxygen tension, Circ. Res., 27:669, 1970.

Einstein, A.: Eine neue Bestimmung der Moleküldimensionen, Ann. Physik., 19:289, 1906.

Folkow, B., Hallbäck, M., Lundgren, Y., and Weiss, L.: Structurally based increase of flow resistance in spontaneously hypertensive rats, Acta Physiol. Scand., 80:93, 1970.

Folkow, B., Hallbäck, M., Lundgren, Y., and Weiss, L.: The effect of intense treatment with hypotensive drugs on structural design of the resistance vessels in spontaneously hypertensive rats, Acta Physiol. Scand., 83:280, 1971.

Folkow, B., Hallbäck, M., Weiss, L., and Lundgren, Y.: The effects of "immunosympathectomy" on blood pressure and vascular "reactivity" in normal and spontaneously hypertensive rats, Acta Physiol. Scand., 84:512, 1972.

Folkow, B., Sonnenschein, R. R., and Wright, D. L.: Loci of neurogenic and metabolic effects on precapillary vessels of skeletal muscle, Acta Physiol. Scand., 81:459, 1970.

Fox, J. R., and Wiederhielm, C. A.: Characteristics of the servo-controlled micropipet pressure system, Microvas. Res., 5:324, 1973.

Friedman, S. M., Nakashima, M., and Mar, M. A.: Morphological assessment of vasoconstriction and vascular hypertrophy in sustained hypertension in the rat, Microvas. Res., 3:416, 1971.

Funaki, S.: Spontaneous spike discharges of vascular smooth muscle, Nature (London), 191:1102, 1961.

Funaki, S.: Electrical and mechanical activity of isolated smooth muscle from the portal vein of the rat, Bibl. Anat., 8:5, 1966.

Fung, Y. C.: Blood flow in the capillary bed, J. Biomech., 2:353, 1969.

Fung, Y. C., and Yin, F.: Peristaltic waves in circular tubes, J. Appl. Mech., September, 1969:579.

Gaehtgens, P., Meiselman, H. J., and Wayland, H.: Erythrocyte flow velocities in mesenteric microvessels of the cat, Microvas. Res., 2:151, 1970.

Granger, H. J., and Shepherd, A. P., Jr.: Intrinsic microvascular control of tissue oxygen delivery, Microvas. Res., 5:49, 1973.

Grodins, F. S.: Computer simulation of cybernetic systems. In: Computers in Biomedical Research, Vol. 1, Stacy, R. W., and Waxman, B. W., Eds. New York: Academic Press, Inc., 1965.

Guyton, A. C., Coleman, T. G., and Granger, H. J.: Circulation: Overall regulation, Ann. Rev. Physiol., 53:13, 1972.

Guyton, A. C., Granger, H. J., and Taylor, R.: Interstitial fluid pressure, Ann. Rev. Physiol., 51:553, 1971.

Harris, P. D., Greenwald, E. K., and Nicoll, P. A.: Neural mechanisms in small vessel response to hemorrhage in the unanesthetized bat, Am. J. Physiol., 218:560, 1970.

Heilbrunn, L. V.: The rheology of protoplasm. In: Flow Properties of Blood, Copley, A. L., and Stainsby, G., Eds. London: Pergamon Press, 1960. pp. 327-331.

Hochmuth, R. M., Marple, R. N., and Sutera, S. P.: Capillary flood flow I: Erythrocyte deformation in glass capillaries, Microvas. Res., 2:409, 1970.

Holman, M. E., and McLean, A.: The innervation of sheep mesenteric veins, J. Physiol., 190:55, 1967.

Honig, C. R.: Control of smooth muscle actomyosin by phosphate and 5'AMP: Possible role in metabolic autoregulation, Microvas. Res., 1:133, 1968.

Honig, C. R.: Control of precapillary sphincters and the mechanisms of circulation-metabolism coupling, Proc. 4th Inter. Cong. Pharmacol., 5:325, 1969.

Intaglietta, M.: Microvascular pressure measurements by cannulation: Independency of concentration gradients and deviation in micro-servonulling, Microvas. Res., 3:396, 1971.

Intaglietta, M.: The measurement of pressure and flow in the micro-circulation, Microvas. Res., 5:357, 1973.

Intaglietta, M., Pawula, R. F., and Tompkins, W. R.: Pressure measurements in the mammalian microcirculation, Microvas. Res., 2:212, 1970.

Intaglietta, M., Richardson, D. R., and Tompkins, W. R.: Blood pressure, flow, and elastic properties in microvessels of cat omentum, Am. J. Physiol., 221:922, 1971.

Intaglietta, M., and Tompkins, W. R.: Micropressure measurement with 1μ and smaller cannulae, Microvas. Res., 3:211, 1971.

Intaglietta, M., Tompkins, W. R., and Richardson, D. R.: Velocity measurements in the microvasculature of the cat omentum by one line method, Microvas. Res., 2:462, 1970.

Jager, N. G.: Electrical model of the human systemic arterial tree. Doctoral Dissertation, University of Utrecht, The Netherlands, 1966.

Johansson, B.: Electromechanical and mechanoelectrical coupling in vascular smooth muscle, Angiologica, 8:129, 1971.

Johansson, B., and Bohr, D. F.: Rhythmic activity in smooth muscle from small subcutaneous arteries, Am. J. Physiol., 210:801, 1966.

Johnson, P. C.: Myogenic nature of increase in intestinal vascular resistance with venous pressure elevation, Circ. Res., 7:992, 1959.

Johnson, P. C.: Autoregulatory responses of cat mesenteric arterioles measured in vivo, Circ. Res., 22:199, 1968.

Johnson, P. C., and Wayland, H.: Regulation of blood flow in single capillaries, Am. J. Physiol., 212:1405, 1971.

Jones, T. W.: Discovery that the veins of the bat's wing (which are furnished with valves) are endowed with rhythmical contractility and that the onward flow of blood is accelerated by each contraction, Phil. Trans. Roy. Soc. London, Part 1, 142:131, 1851.

Källskog, Ö.: Single glomerular blood flow as measured with carbonized 141-Ce labelled microshperes, Acta Physiol. Scand., 85:408, 1972.

Katchalsky, A., Kedem, O., Klibansky, C., and de Vries, A.: Rheological considerations of the haemolysing red blood cell. In: Flow Properties of Blood, Copley, A. L., and Stainsby, G., Eds. London: Pergamon Press, 1960. pp. 155-171.

Lee, J. S., and Fung, Y. C.: Modeling experiments of a single red blood cell moving in a capillary blood vessel, Microvas. Res., 1:221, 1969.

Lew, H. S., and Fung, Y. C.: The motion of the plasma between the red cells in the bolus flow, Biorheology, 6:109, 1969.

Lew, H. S., and Fung, Y. C.: Plug effect of erythrocytes in capillary blood vessels, Biophys. J., 10:80, 1970.

Loh, D. von: The effect of adrenergic drugs on spontaneously active vascular smooth muscle studied by long term intracellular recording of membrane-potential, Angiologica, 8:144, 1971.

Lundholm, L., and Mohme-Lundholm, E.: Length at inactivated contractile elements, length tension diagram, active state and tone of vascular smooth muscle, Acta Physiol. Scand, 68:347, 1966.

Mall, F.: Die Blut-und Lymphwege in Dunndarm des Hundes, Ber. Sachs. Ges. (Akad) Wiss., 14:151, 1888.

McCuskey, R. S.: Sphincters in the microvascular system, Microvas. Res., 3:428, 1971.

Mechedlishvillie, G. I.: Vascular Mechanisms of the Brain. New York: Consultants Bureau, a Division of Pergamon Press, 1969.

Mela, M. J.: Elastic-mathematical theory of cells and mitochondria in swelling process, Biophys. J., 8:83, 1968.

Mellander, S.: Systemic circulation: Local control, Ann. Rev. Physiol., 32:313, 1970.

Mellander, S.: Internation of local and nervous factors in vascular control, Angiologica, 8:187, 1971.

Merrill, E. W.: Rheology of blood, Physiol. Rev., 49:863, 1969.

Nicoll, P. A.: Intrinsic regulation in the microcirculation based on direct pressure measurements. In: The Microcirculation, Winters, W. L., and Brest, A. N., Eds. Springfield, Ill.: Thomas, 1969. pp. 89-101.

Nicoll, P. A., and Webb, R. L.: Blood circulation in the subcutaneous tissue of the living bat's wing, Ann. N. Y. Acad. Sci., 46:697, 1946.

Nicoll, P. A., and Webb, R. L.: Vascular patterns and active vasomotion as determiners of flow through minute vessels, Angiology, 6:291, 1955.

Noordergraaf, A.: Development of an analog computer for the human systemic arterial system. In: Circulatory Analog Computers, Noordergraaf, A., Jager, G. N., and Westerhof, N., Eds. Amsterdam: North Holland Publishers, 1966.

Noordergraaf, A.: Hemodynamics. In: Biological Engineering, Schwan, H. P., Ed. New York: McGraw-Hill Book Company, 1969. pp. 391-545.

Noordergraaf, A., and Horeman, H. W.: Numerical evaluation of volume pulsations in man, Physics in Med. and Biol., 3:59, 1958.

Noordergraaf, A., Horeman, H. W., and Vierhout, R.: Theory of elasticity of blood vessels especially concerning the influence of the thickness of the wall. University of Utrecht, Physics Lab., Int. Report V1376, Utrecht, 1956.

Pater, L. de: An electrical analogue of the human circulatory system. Doctoral Thesis, University of Groningen, The Netherlands, 1966.

Peterson, L. H.: Properties and behavior of living vascular wall, Physiol. Rev., 42:309, 1962.

Peterson, L. H.: Physical factors which influence vascular caliber and blood flow, Circ. Res. (Suppl. I), 18:3, 1966.

Raper, A. J., and Peterson, L. H.: In vivo geometry and mechanical properties of small mesenteric arteries, Bibl. Anat. 10:288, 1968.

Renkin, E. M., and Rossel, S.: Independent sympathetic vasoconstrictor innervation of arterioles and precapillary sphincter, Acta Physiol. Scand., 54:381, 1962.

Rhodin, J. A. G.: The ultrastructure of mammalian arterioles and precapillary sphincters, J. Ultrastruc. Res., 18:181, 1967.

Rhodin, J. A. G.: Ultrastructure of mammalian venous capillaries, venules, and small collecting veins, J. Ultrastruc. Res., 25:452, 1968.

Richardson, D. R., and Zweifach, B. W.: Pressure relationships in the macro- and microcirculation of the mesentery, Microvas. Res., 2:474, 1970.

Shapiro, A. H., Jaffrin, M. Y., and Weinberg, S. L.: Peristaltic pumping with long wave lengths at low Reynolds number, J. Fluid Mech., 37:799, 1969.

Smaje, L., Zweifach, B. W., and Intaglietta, M.: Micropressures and capillary coefficients in single vessels of the cremaster muscle of the rat, Microvas. Res., 2:96, 1970.

Somlyo, A. P., and Somlyo, A. V.: Vascular smooth muscle, Pharmacol. Rev., 20:197, 1968.

Stainsby, W. N.: Local control of regional blood flow, Ann. Rev. Physiol., 35:151, 1973.

Sutera, S. P., and Hochmuth, R. M.: Large scale modeling of blood flow in the capillaries, Biorheology, 5:45, 1968.

Sutera, S. P., Seshardi, V. A., Croce, P. A., and Hochmuth, R. M.: Capillary blood flow II: Deformable model cells in tube flow, Microvas. Res., 2:420, 1970.

Topham, W. S., and Warner, H. R.: The control of cardiac output during exercise. In: Physical Basis of Circulatory Transport, Reeve, E. B., and Guyton, A. C., Eds. Philadelphia: W. B. Saunders Company, 1967. pp. 77-90.

Warner, H. R.: Control of heart function, Proc. 20th Ann. Conf. Eng. in Med. and Biol., 9:11.6, 1967.

Wayland, H.: Photosensor method of flow measurement in the microcirculation, Microvas. Res., 5:336, 1973.

Wayland, H., and Johnson, P. C.: Erythrocyte velocity measurement in microvessels by a two-slit photometric method, J. Appl. Physiol., 22:333, 1967.

Weil, M., and Shubin, H.: Changes in venous capacitance during cardiogenic shock - a search for the third dimension, Am. J. Cardiol., 26:613, 1970.

Wells, H. S., Youmans, J. B., and Miller, S. L.: Tissue pressure (intracutaneous, subcutaneous, and intramuscular), as related to venous pressure, capillary filtration, and other factors, J. Clin. Invest., 17:489, 1938.

Wells, L. A.: Circulatory patterns of hibernators, Am. J. Physiol., 221:1517, 1971.

Westerhof, N., and Noordergraaf, A.: Arterial viscoelasticity: A generalized model, J. Biomech., 3:357, 1971.

Wiedeman, M. P.: Effect of denervation on diameter and reactivity of arteries in the bat wing, Circ. Res., 3:618, 1955.

Wiedeman, M. P.: Lengths and diameters of peripheral arterial vessels in the living animal, Circ. Res., 10:686, 1962.

Wiedeman, M. P.: Dimensions of blood vessels from distributing artery to collecting vein, Circ. Res., 12:375, 1963.

Wiedeman, M. P.: Contractile activity of arterioles in the bat wing during intraluminal pressure changes, Circ. Res. 19:559, 1966.

Wiedeman, M. P.: Blood flow through terminal arterial vessels after denervation of the bat wing, Circ. Res., 22:83, 1968.

Wiederhielm, C. A.: Distensibility characteristics of small blood vessels, Fed. Proc., 24:1075, 1965.

Wiederhielm, C. A.: Effects of temperature and transmural pressure on contractile activity of vascular smooth muscle, Bibl. Anat., 9: 321, 1967.

Wiederhielm, C. A.: Dynamics of transcapillary fluid exchange. In: Biological Interfaces: Flows and Exchanges. Boston: Little, Brown and Company, 1968. pp. 29-63.

Wiederhielm, C. A.: The interstitial space and lymphatic pressures in the bat wing. In: The Pulmonary Circulation and Interstitial Space, Fishman, A. P., Ed. Chicago: University of Chicago Press, 1969. pp. 29-40.

Zweifach, B. W.: General principles governing the behavior of the microcirculation, Am. J. Med., 12:684, 1957.

Zweifach, B. W.: Local regulation of capillary pressure, Circ. Res. (Suppl. I), 28:1, 1971.

Zweifach, B. W., and Intaglietta, M.: Mechanics of fluid movement across single capillaries in the rabbit, Microvas. Res., 1:83, 1968.

CHAPTER ONE... INTRODUCTION

I. The Circulation

A proper definition of the circulatory system includes the cardiovascular system (e.g., heart, blood vessels, blood, etc.), as well as those organ and body subsystem functions which influence and control the properties and behavior of the circulation. One of the principal functions traditionally ascribed to the circulatory system is to provide and maintain a cellular environment which is appropriate for the needs of each part of the body. The life sustaining constituents of the red cells and plasma are brought into proximity to the target cells and metabolic products removed via an exquisite system of vessels. Conceptually this system of vessels may be divided into two regions, the macrovasculature ("large" distributing arteries and "large" collecting veins), and the microvasculature. The general subject of this dissertation is the microvasculature and the flow within it, the microcirculation.

Though there is no standard definition of the microvasculature, it is generally accepted that the capillaries are part of it, but the boundaries both on the arterial and venous sides are not clear-cut. A major reason for the lack of definition is the variability in the criteria which have been applied. Vessel anatomy, structure, function, character of fluid flow, and mode of regulation have each been utilized to specify vessel types and to help delineate boundaries.

For the purpose of the present discussion, a

microcirculatory bed refers to that region of the circulation extending from small artery to small vein. Small artery refers to the smallest vessel in a repetitive branching sequence of arteries which structurally still retains an intima, media (at least two layers of smooth muscle cells), and an adventitia, and which gives rise to arterioles as side branches. Small veins are those vessels which are fed by muscular venules, the smallest venous vessel which possesses distinct muscle cells. In between the small artery and vein lie the arterioles, metarterioles (mesentery), terminal arterioles, pre capillaries, capillaries, nonmuscular or post capillary venules and muscular venules. This is a working definition which would need to be modified for specific vascular beds. The exchange between intravascular and extracellular constituents occurs principally through the walls of the smallest of these vessels, the capillaries (there is some recent evidence of oxygen exchange in the arterioles and bulk exchange in the post capillary venules; Duling, 1972). Because different parts of the body have different structure and function, their circulatory requirements are different. In addition, the same part of the body may have different needs at different times. Thus, the circulatory system is required to sense these differences and changes in circulatory requirements and respond in such a way as to maintain an appropriate cellular environment. To accomplish this, there is present an elaborate system of circulatory controls. These may conceptually be divided into local and system controls.

In figure 1.1 a descriptive model depicting local

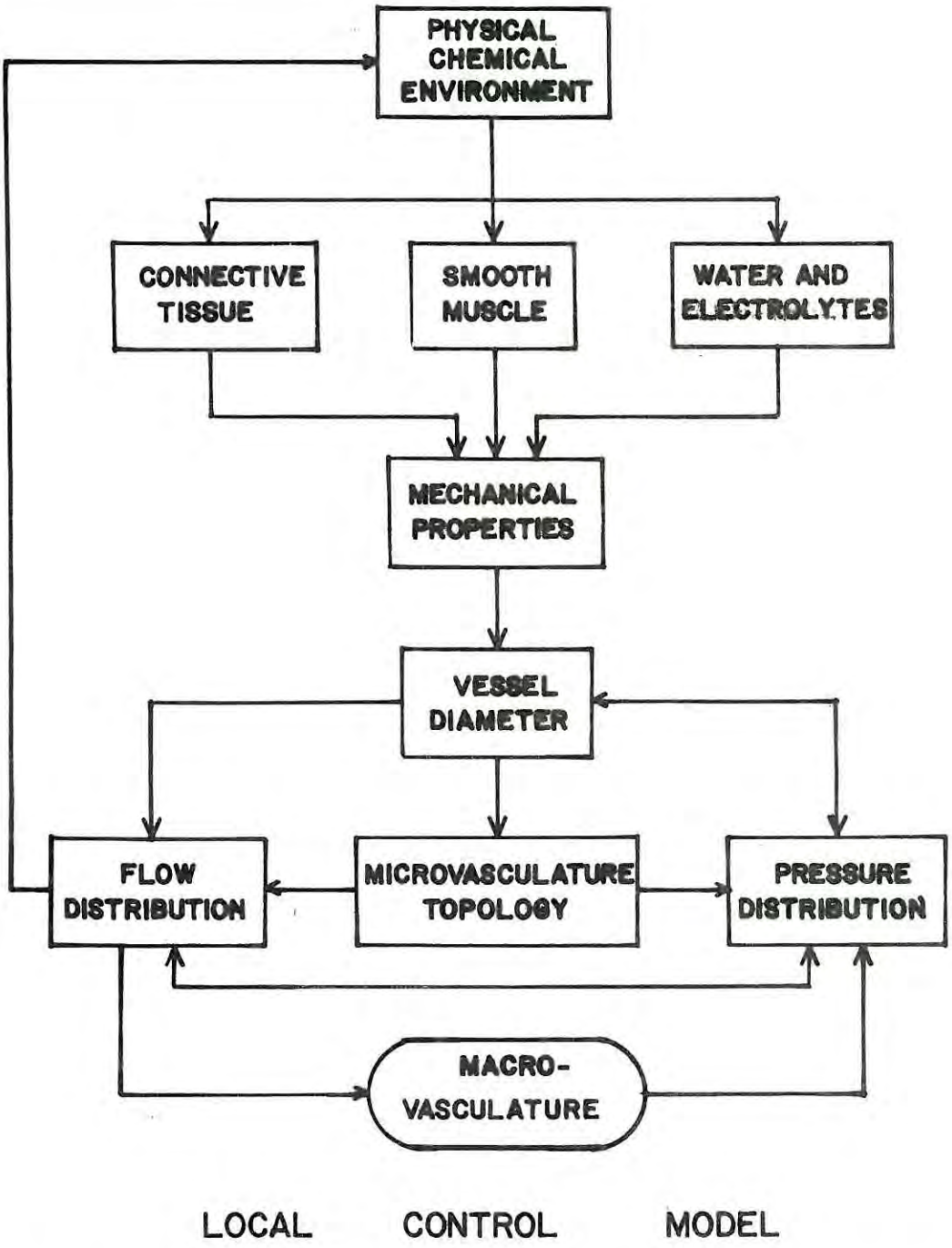

Figure 1.1. Descriptive representation of the general characteristics of local control. Local control is mediated through the diameter of microvessels which are in turn determined by their mechanical properties. Control is effected through the blood vessel wall smooth muscle, connective tissue, and water and electrolyte contents by their physical-chemical environment. The control in turn affects the topology of the microvasculature and the distribution of pressure and flow within it.

microcirculatory control is shown. One of the factors of importance in this control process is the mechanical properties of the vessels of the microvasculature. These mechanical properties which significantly influence vessel diameter are dependent on the vessel wall constituents, including the water and the electrolyte content, contractile state of vascular smooth muscle, and connective tissue properties. Each of these quantities is, in turn, dependent on the physical and chemical environment to which the vessel is exposed. The physical and chemical environment is itself dependent on the flow distribution in addition to special local factors which are mainly related to metabolism and properties of specific beds, e.g., potassium in active skeletal muscle, adenosine in heart muscle, etc.

The flow distribution is determined by a number of factors. The microvasculature topology, which refers to the manner in which the various vessels of the microvasculature are anatomically and functionally spatially arranged, has a direct influence on flow and flow distribution. A specific topology in part determines the pressure distribution which also has a direct influence on flow distribution. In addition, the influence of pressure distribution and vessel mechanical properties acting on vessel diameter represent another pathway for the control of flow distribution. Both pressure and flow depend on the interaction with the microvasculature. A more detailed description of this interaction between the micro- and macrovasculature in addition to the interaction of local and system controls is shown in figure 1.2. In figure 1.2, an attempt is made

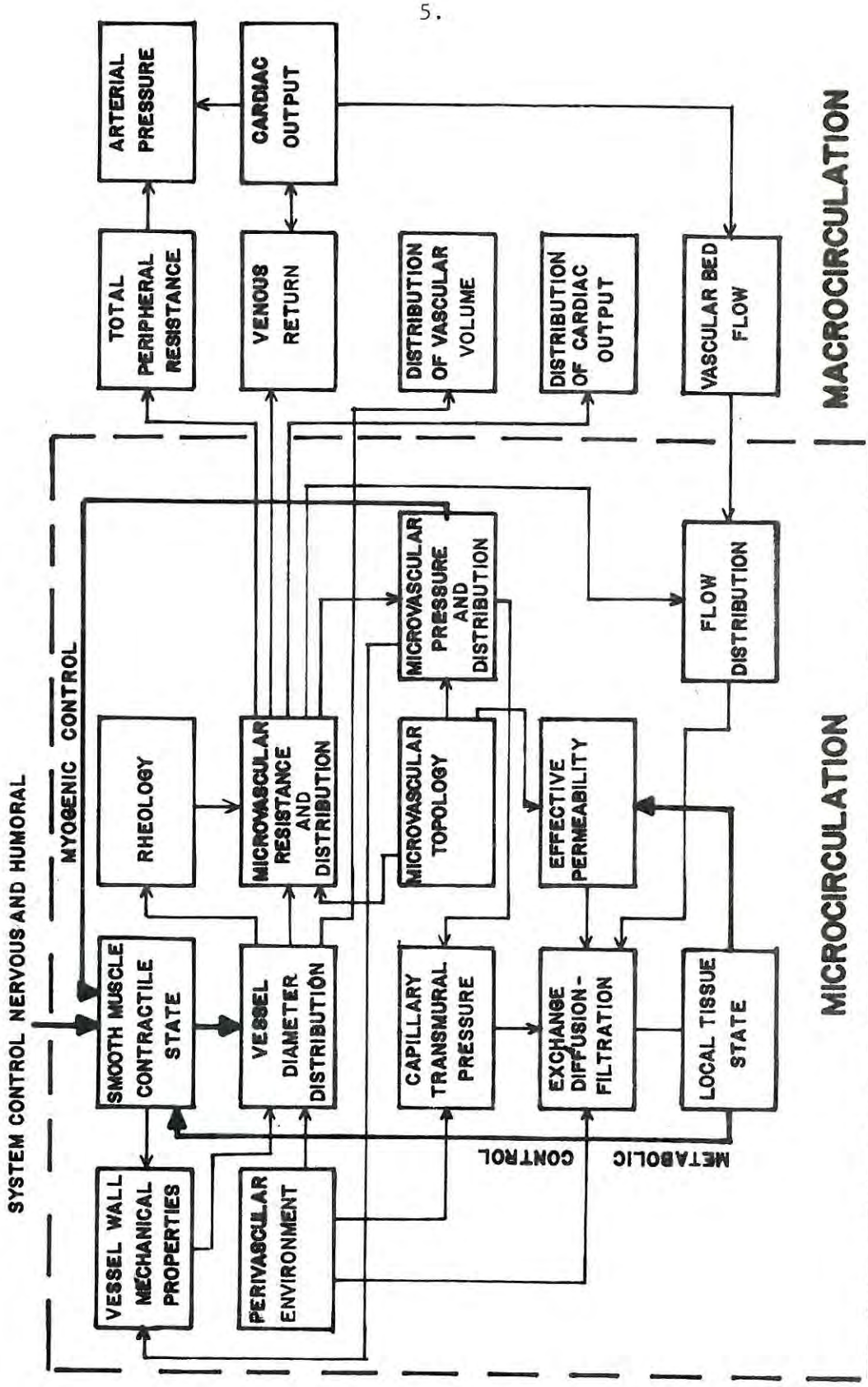

Figure 1.2. Descriptive model of interaction between microcirculation and macrocirculation.

to provide a conceptual framework from which the role of the microvasculature may be viewed in perspective. Several functional concepts are illustrated in this descriptive model. It shows the interrelationship between local microcirculatory facets (e.g., topology, rheology, diameter distribution, etc.) and the manner in which these facets influence important microcirculatory parameters (e.g., pressure distribution, exchange, local tissue state, etc.). It also depicts the interdependency of the microcirculatory and macrocirculatory parameters and illustrates the interaction of local and system controls.

Thus, the function of the microcirculation in the scheme of the total circulatory system is three-fold. Each microcirculatory bed is required to function in accordance with its local tissue requirements, which relate to fluid balance, tissue nutrition, and catabolite removal, i.e., local function. In addition, certain microcirculatory beds are also required to function as controllers in accordance with the requirements of other microcirculatory beds, i.e., system control requirements. This is especially evident in those vascular beds which serve, for example, the endocrine glands, kidney, brain and other organs which either secrete or respond to changes in circulatory status. The third aspect of microvascular function is related to its resistive or peripheral load characteristic. The microvasculature as herein defined is responsible for a substantial part of the total vascular resistance of a given vascular bed. Since the composite of individual bed resistances

together with cardiac output determine arterial pressure and their relative values determine cardiac output distribution, it is clear that the resistance characteristic is an important local and system functional parameter.

II. The General Problem

This dissertation is concerned with the experimental and theoretical study of two of these microcirculatory functional aspects: the resistive or peripheral load characteristic of the microvasculature and the hemodynamics within the microvasculature as it relates to local function. The initial motivation for the present research began some years ago while the author was engaged in quite a different activity. It is felt to be useful to briefly describe these earlier events, as they have a direct bearing on the specific goals of the present work to be described shortly (section III).

Some years ago the author was participating in a study related to the evaluation of artificial circulatory assist devices. Among the various devices for which evaluation was planned was the artificial heart. One of the criteria for acceptance of such a device is its ability to produce an appropriate outflow over a broad range of load conditions. The resistive part of this load is the total peripheral resistance (TPR), and it is this quantity which is a most important component of the total load with respect to pump energy expenditure.

In order to test for proper operation design, it was necessary to determine the expected upper and lower bounds on TPR for a variety of physiologic and pathologic circulatory states. While attempting to do this, it became apparent that though there was sufficient experimental data in the literature to make

reasonable estimates of these limits, there was no obvious way to express TPR or for that matter any of the vascular bed resistances in terms of fundamental quantities. This total reliance on empirical data provoked a search for an alternate approach.

It occurred to the author that the problem of representing the resistance characteristic of the microvasculature needs to be dealt with when attempting to model or simulate the circulatory system. Turning to that body of literature, it was found that the "problem" had been handled quite simply. Starting with a conceptual view of the vasculature tree as an assemblage of vascular beds, each of which makes its own contribution to TPR, a number of workers had represented the systemic vasculature (Noordergraaf, 1956; Attinger, 1966; De Pater, 1966; Jager, 1966; Westerhof, 1969) or developed closed loop circulatory system representations (Grodins, 1965; Topham, 1966; Warner, 1967; Beneken, 1967; Guyton, 1972; Peterson, 1973). In each case, however, the microvasculature is represented by a subsystem model which is usually a resistance or resistance and compliance which terminates the vascular tree in a passive and in some cases in a variable fashion.

Thus, for each vascular bed included in the system models, the microvasculature and microcirculation are included as part of a phenomenological description of the overall bed hemodynamics. Though these circulatory models had proved to be useful in characterizing and analyzing a number of aspects of circulatory function, it appeared that the simplified microvascular representation would

ultimately limit the usefulness of an otherwise powerful tool, since the physiological properties of the microvasculature were not characterized in terms of its physical properties. At this point it was felt that since it was possible to identify the microvascular factors upon which vascular bed resistance most critically depended (see for example figure 1.2), it should be possible to develop at least a reasonable quantitative formulation. It seemed clear even at this stage that a suitable formulation should take into account the microvascular topology, dimensions and the mechanical and other physical properties of the individual arterial vessels, as well as their perivascular environment. A search of the microcirculatory literature revealed that the kind of detailed topological information needed was quite scarce. Only one specific vascular region had been studied in vivo in sufficient detail for the present purpose. In a series of papers (Wiedeman, 1962, 1963) there could be found a description of the topology and dimensions of the vessels of the wing of the small brown bat. These could serve as a basic anatomical framework or prototype geometric configuration needed for a microvasculature characterization. [Since that time similar data on the mesentery vasculature (Zweifach, 1971) and muscle vasculature (Folkow, 1972) have been published.]

The advantage of Wiedeman's data over the data of Green (1944) which he calculated from Mall's data (1888) is two-fold. First, the bat wing data are obtained from a living and undisturbed animal preparation. Mall's original data were for fixed vessels of

the dog mesentery. Secondly, the wing could provide an experimental preparation for further study if necessary.

A further review of the microcirculatory literature showed the existence of a large body of pertinent experimental and theoretical information relevant to microcirculatory properties and function. But, in general, because each investigator had been principally interested in one or two aspects of microcirculatory function, the information, though relevant, existed in a scattered, non-cohesive array. Thus, for example, experimental work had been done to explain and characterize the anomalous viscosity and general rheologic properties of blood in small vessels (Bayliss, 1960; Copely, 1960; Charin, 1967; Merril, 1969). The mechanical properties of the erythrocytes themselves had also been studied (Canham, et al., 1971; Hochmuth et al., 1972). Blood flow in the smallest vessels, the capillaries, had been analyzed theoretically (Bernard et al., 1968; Fung, 1968; Lighthill, 1968; Fitz-Gerald, 1969), studied using hydrodynamic models in vitro (Sutera and Hochmuth, 1968; Lee and Fung, 1969; Sutera et al., 1970), and in vivo experimental data obtained (Johnson and Wayland, 1967; Harris et al., 1968; Johnson, 1971). Flow in microvessels other than the capillaries had received little theoretical treatment, but experimental in vivo data regarding pressures and velocities in the mesentery (Intaglietta et al., 1970; Richardson and Zweifach, 1970: Gaehtgens et al., 1970; Zweifach, 1972) were fairly extensive. The morphology and topology of the vessels constituting the microvasculature had been studied and

documented (Nicoll and Webb, 1955; Wiedeman, 1962; Rhodin, 1967; Zweifach, 1972). In addition, experimental data related to the *in vivo* mechanical properties of these vessels (Wiederhelm, 1967, 1969; Raper and Peterson, 1968; Baez, 1968, 1969; Oka, 1971), vascular smooth muscle function (Lundholm, 1966; Somlyo and Somlyo, 1968; Speden, 1968; Johansson, 1971) and their control (Duling *et al.*, 1968; Folkow *et al.*, 1970; Mellander, 1971; von Loh, 1971; Granger and Shepard, 1972; Zweifach, 1973) had been obtained. The list is quite long, but the point that is important is that to be useful for characterizing the integrated nature of the microvasculature, an appropriate structuring of this kind of information would be required.

Thus, one group of literature revealed the presence of circulatory system models with quite simplified microvascular representations, and another group of literature revealed the existence of an array of unstructured specific microvascular data. The absence of an adequate peripheral load characterization of the microvasculature was thus revealed to be just one aspect of a generalized void or gap that needed to be filled.

Another aspect of the void in our understanding became apparent in studying the microcirculatory literature and particularly that dealing with the bat wing. The author became interested in the "inner" workings of the microvasculature, that is, the microcirculation itself. Particularly intriguing were the descriptions of vessel dynamics, spontaneous rhythmical variations in small vessel

diameters which were especially prominent in post capillary microvasculature. The post capillary dynamics were observed by Jones (1851) and later elaborated on by Nicoll and Webb (1946), Wiedeman (1966) and most recently D'Argrosa (1971). Such rhythmical variations in diameter are not limited to the bat wing, for similar dynamics have been reported in a number of species, including the dog hind limb (Johansson et al., 1966), chicken embryo (Attardi, 1955), mammalian portal vein (Axelsson, 1962; Booz, 1963); mesenteric vein (Cuthbert, 1966; Holman, 1967), and skin venules of the frog (Funaki, 1961). What role do these dynamics play in the function and control of the circulation? This is not just an academic question. The importance of the post capillary region of the microvasculature from a local and systems point of view partially resides in the fact that it serves simultaneously to 1) accommodate inflow from a dispersed capillary vasculature, 2) store a considerable portion of the total blood volume, and 3) provide the initial pathways for blood return to the heart. In spite of its significance, this region has been studied with much less intensity than the corresponding pre capillary vessels. The complexity of the topology, existence of valves, suggested rheologic implications in this low velocity region and the presence of apparently complex mechanisms of control such as described above are among those factors which need to be characterized and understood if we are to further clarify and understand this region of the microvasculature. In view of the general characteristics of this region of the circulation, a

particularly pertinent and interesting question is the hemodynamic significance of the observed rhythmic variation in vessel diameter.

These changes in caliber which bear no obvious relationship to the periodicities of either heart rate or respiration have been assigned the name venomotion. Venomotion probably represents the most prominent aspect (as observed through the microscope) of the post capillary vasculature in the experimental animal directly used in these studies. The fundamental nature, in vivo characteristics, and functional significance of venomotion have been the subject of both speculation and some experimental study. Because of its potential significance as an important capillary control mechanism and to evaluate previous speculation concerning its in vivo characteristics, venomotion and its associated interaction with capillary and pre capillary dynamics became of considerable interest to this author. It was thought that one way to help gain insight into the consequences of these dynamics would be to suitably represent them in mathematical form. But representation of a single dynamic process without including the effects and interactions of the complex geometrical and physical environment would, it was felt, not yield the kind of understanding that was needed.

Two basic areas of inquiry had now evolved. One related to the peripheral load characteristic of the microvasculature, and the other concerned the relationship between microvascular dynamics and blood circulation. To represent the peripheral load characteristic an appropriate characterization of the microvasculature,

which considered its topology, properties of the vessels and their environment, blood rheology, and individual vessel hemodynamics, is necessary. And to understand hemodynamic interactions within the microvasculature a suitable representation of the dynamics together with the physical characteristics of the environment in which they occur is necessary. It seemed, therefore, that if a suitable microvascular characterization could be developed, it would provide the necessary framework to aid in the study and understanding of both of these aspects. In point of fact, it appeared that neither the resistive function nor the local hemodynamics could be adequately studied without the inclusion of pertinent aspects of the other.

III. Specific Goals

One of the tools which is used to aid in the process of understanding systems dominated by complex interactions, as is the case within the microvasculature, is the development and use of models. A model as used here is a quantified, unified representation of those factors (e.g., topology, vessel properties, rheology, hemodynamics) and their interrelationships which are pertinent to those functions and performance characteristics being studied. The overall goal of this dissertation is to develop a microvascular characterization or model in which the physiological properties and behavior of a vascular bed are represented in terms of the physical properties and dynamics processes within the microvasculature and further to utilize the model, together with appropriate experimental studies, to enhance our understanding of microcirculatory hemodynamics and function. The purpose in developing such a model is to aid in the study and understanding of two specific aspects of the microvasculature. The first of these is to help clarify the relationship between the microvascular properties of a vascular bed and the macroscopically measured vascular resistance. The second is to increase our understanding of the way in which vascular dynamics such as venous venomotion and arteriole vasomotion separately and together influence hemodynamics and function within the microvasculature.

In addition to these specific objectives, the development of a microvascular model of the type envisioned represents an initial and hopefully substantial advance over previous methods of

representing the microvasculature. It thus may provide a tool from which insight into the integrated behavior of the microcirculation may be gained in a manner not otherwise possible. Secondly, it may serve as a prototype model for use in conjunction with circulatory system models to enhance their utility in studying the local-system interactions as well as physiological and pathological processes for which the properties and behavior of the microvasculature are of special importance.

CHAPTER TWO... VASCULAR BED RESISTANCE IN TERMS OF MICROVASCULAR PARAMETERS

I. Introduction

In this chapter the question of how to characterize the microvasculature so as to predict the vascular bed resistance in terms of microvascular parameters is considered. The purpose is to use the characterization so obtained to provide information on the resistance distribution throughout the vascular bed. Such information is a vital part of the process of developing a microvascular model suitable for studying the microcirculation and its interaction with the macrovasculature.

The experimental preparation chosen for the initial effort was the vasculature of the wing of the little brown bat (myotis Lucifugis). There are a number of reasons for this choice, the most relevant to the present work being the following:

(1) The entire vasculature from main artery entering the wing from the shoulder to the main vein leaving may be observed without the introduction of any anesthetics or other functionally depressing or traumatic interventions.

(2) There is a reasonable anatomical correspondence of the wing vasculature to the subclavian vascular bed.

(3) The wing vasculature possesses a number of facets which appear to be quite general in the sense that they would appear to be common to other vascular beds and to other animals. This includes the topology, characteristics of fluid flow, and aspects of vessel

structure. In addition, it provides the potential for separating the subclavian bed into its two components of skin and muscle. The skin corresponds to the membrane and overlying epidermis and the muscle flow to the phalanges and associated skeletal muscle.

(4) Removal of nervous control is easily effected by sectioning the major nerve which arises from the brachial plexus and enters the wing at the shoulder.

(5) Some of the topology of the vasculature had already been well documented in the literature, and that which remained to be done for the present purposes could be accomplished to effect the necessary total topological description.

The general approach in dealing with the microvasculature is to view it as a complex subsystem of the total circulatory system. The overall characteristics of each such subsystem depend upon an array of interrelated factors. Five descriptive terms (facets) are used as a convenient method of characterizing groups of these factors for any vascular bed. These five facets are:

(1) Topology and architecture;

(2) Structure and physical properties;

(3) Fluid properties;

(4) Fluid dynamics;

(5) Control.

The general problem is to systematically quantify each of these facets and then characterize their interrelationships so that the composite representation reflects the essential features of the microvasculature.

The first phase of the characterization process is to represent the dimensional and topological characteristics of the vascular bed in a form which serves as a basic framework for a microvascular model. Thus the main emphasis of this chapter is to characterize and structure the vascular bed in a form which may be termed the "system to be controlled". For this purpose three of the above facets are dealt with in detail, while two others are included in a later chapter (Chapter Four). To be included in detail here are: (1) Topology and architecture (section II-A), (3) Fluid properties, and (4) Fluid dynamics. Because facets (3) and (4) are inherently coupled from an analysis viewpoint, these are combined and treated under the heading of hemodynamics (section II-C). The method of initially dealing with vessel structure and physical properties (facet 2) is discussed in section II-A, but inclusion of intrinsic control (facet 5) remains absent from the essentially topological model to be developed in this chapter. However, a more extensive characterization of pertinent aspects of vascular control shall be presented in Chapter Four where arteriole vasomotion and venous venomotion are incorporated into a microvascular model.

II. Characterization of the Vascular Facets

A. Topology and Architecture

Topology refers to the manner in which the various vessel types which constitute the vasculature are spatially arranged. The detailing of the topology of the bat wing is in large measure due to Wiedeman (1962,1963). The terminology and definitions she employed are used here. Two aspects of the topology not previously documented are the branching sequences arising from the main arterial vessels and a clear distinction between arterioles and terminal arterioles (as defined by Wiedeman).

Architecture refers to the dimensions of individual vessels and the nature of their interconnection, including the characteristics of the junctional region at branch points. Such regions are frequently observed to be stenotic for short distances at the arterial branch entrances and to be guarded by valves in the post capillary vasculature.

1. Experimental Data

In order to obtain a relatively complete description of the topology and architecture of the experimental model, a series of experiments, primarily observational in nature, was carried out. Primary emphasis was on the two as yet undocumented regions described above.

The bat wing was prepared for observation in a standard fashion (Wiedeman, 1962). Briefly, the body of the bat is placed within a lucite chamber with provision for adequate ventilation. The chamber is mounted on top of a transparent board, and a

wing is stretched over the board and held in place by two or three clamps placed so as not to interfere with the circulation. The board assembly is then placed on the microscope stage, and the microscope image with magnifications up to 1200X is displayed on a closed circuit television monitor. In some instances the TV camera is replaced with a cine camera and films taken at framing rates from 16 to 64 frames per second. The experimental setup also had the capability for video recording. Using this method it was possible to measure vessel lengths and diameters with an accuracy of about one micron. The inside diameter is clearly visible as the boundary between the vessel wall and the flowing blood within the vessel lumen.

The main arterial vessels entering the wing were followed from their entrance until their termination at peripheral sites on the wing surface. The inside diameters of the vessels were measured at various longitudinal sites, and the branching sequence recorded, including the number of branches, and the length between adjacent branches in addition to major bifurcation sites. At these sites the inside diameters of the parent vessel and of the two vessels constituting the fork were recorded. A typical vascular topology of the main artery and its branches is indicated in figure 2.1. Terminal arterioles were distinguished from arterioles in a manner indicated in figure 2.2, which shows the several vessel types and their interrelationships in schematic form. The vessel labeled main artery in figure 2.2 corresponds to the main vessel of figure 2.1. The 57 micron branch is located at the site of the arrow in

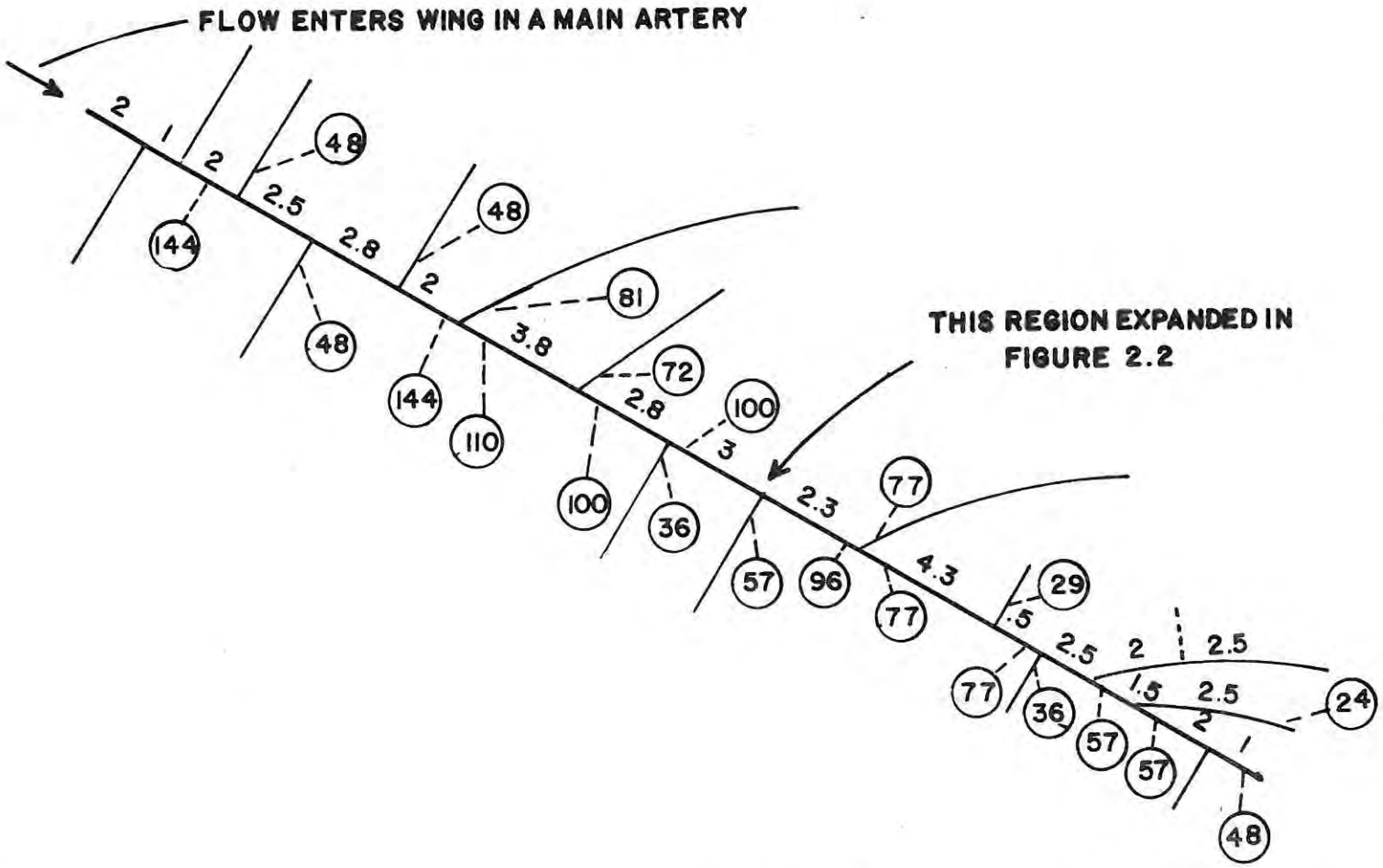

Figure 2.1. Representative main arterial topology. Circled numbers are vessel internal diameters in microns. Uncircled numbers are lengths between branches of main artery in millimeters.

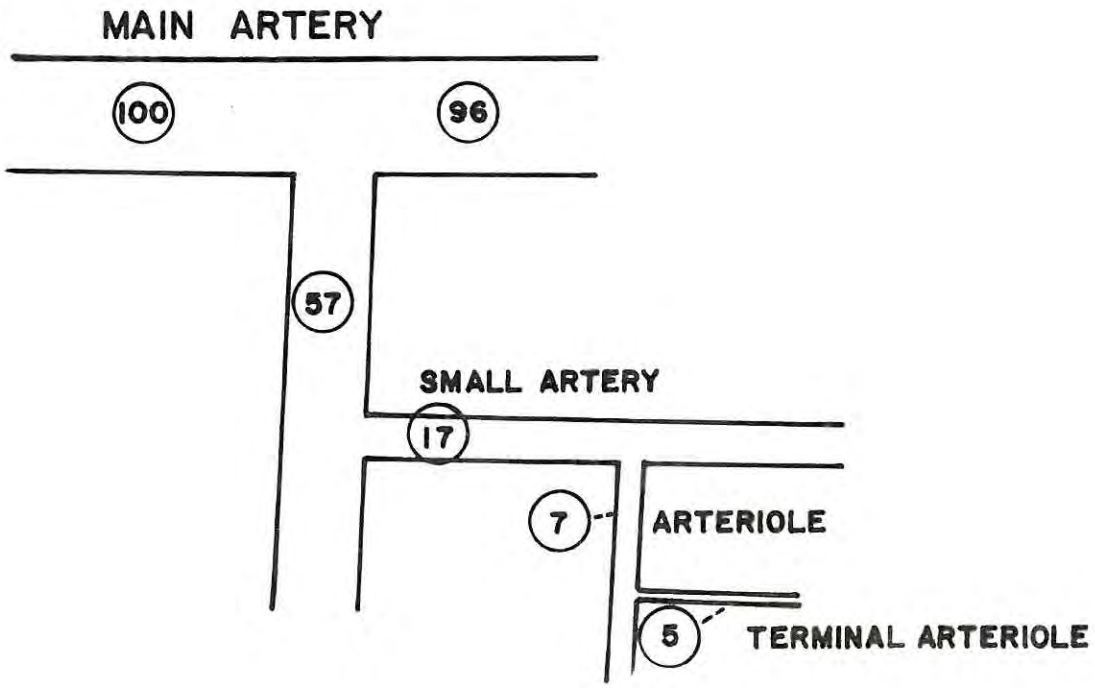

Figure 2.2. Detail of branching sequence from main artery to terminal arteriole. Circled numbers are inside diameters in microns.

figure 2.1. The terminal arteriole may be seen to be the final arterial branching vessel prior to a capillary or capillary mesh.

The results of the present observation together with those of Wiedeman (1962,1963) are shown in table 2.1.

Table 2.1. Vessel diameters (microns), lengths (mm), and average number of branches used to construct topological model.

vessel	average diameter	length	number of branches
Main artery	97.0	36.0	13.0
Artery	52.0	17.0	12.0
Small artery	19.0	3.5	9.7
Arteriole	7.0	.95	4.6
Terminal arteriole	5.0	.20	3.1
Capillary	3.7	.23	-
Post capillary venule	7.3	.21	-
Venule	21.0	1.0	5.0
Small vein	37.0	3.4	14.1
Vein	76.0	17.6	24.5

The body of numerical data contained in table 2.1 forms the basis for constructing the initial topological and architectural representation of the vasculature. Figure 2.3 is the schematic representation of the topological pattern used to characterize and analyze the vasculature. It may be thought of as a "first generation" or topological model.

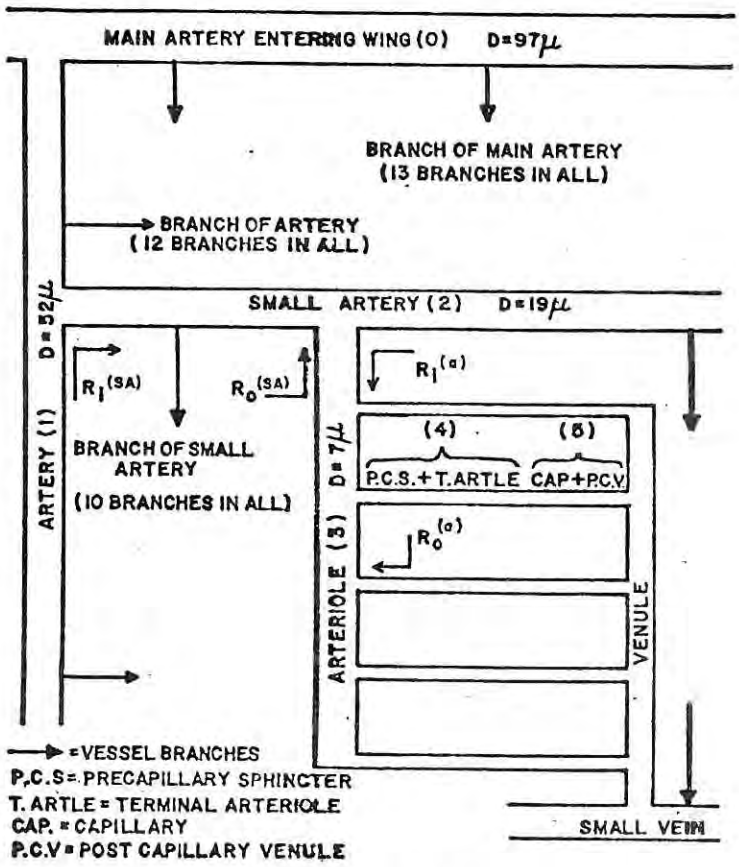

Figure 2.3. TOPOLOGICAL MODEL

VESSEL NAMES ARE THOSE ORIGINALLY PUT FORWARD BY WIEDEMAN (1962). NUMBERS IN PARANTHESIS DESIGNATE VESSEL ORDER OF BRANCHING

In this figure one pathway from the main artery to the small vein is shown in detail, and the remainder of the branches and vascular pathways are shown as straight arrows. Each vessel is given a name in accordance with those put forward by Wiedeman (1962). In addition, a branching order designation is shown in parentheses. The quantities R_i and R_o correspond to the input and output impedance at a given branching level. Thus for example $R_i^{(SA)}$ is the input impedance seen looking into the small artery, whereas $R_o^{(SA)}$ is the output impedance seen looking back into the small artery from the arteriole. In terms of the branching order designation to be used in subsequent figures (e.g., figure 2.6), these impedances may be equivalently written as $R_i^{(2)}$ and $R_o^{(2)}$, respectively. D is the average vessel inside diameter.

Thus using the present results together with those of Wiedeman provides the detailed topological and architectural data required. The real topology is used as a reference, and a number of assumptions are made in order to develop a reduced but representative vascular structure. In the reduced version, the average vessel dimensions and branching distributions are maintained. The principal difference between the real topology and its reduced representation for analytical purposes is the way in which arcuate vessels are represented.

2. Topological Model

Starting with the main artery at the top of figure 2.3, a single pathway is illustrated in detail to the venule with the remaining pathways represented in the figure by the large arrows. Adjacent to the name of each vessel type is a number in parenthesis. This is for reference purposes and may be termed the vessel branching "order". There are a number of assumptions which are intrinsic to the topological model. These are the following:

(1) Small arteries arise only from arteries.

(2) All small arteries terminate at the point where two forward flows merge as the result of joining with another small artery which arose from an adjacent artery.

(3) Arterioles arise only as side branches of small arteries.

(4) Terminal arterioles arise only as side branches of arterioles and terminate into a capillary or capillary net.

(5) Capillaries arise as the final ramification of the terminal arterioles and terminate in post capillary venules.

(6) Post capillary venules draining capillaries from the same parent terminal arteriole, drain into the same venule.

Assumption (1) is consistent with experimental observations. Assumption (2) excludes the possibility that small arteries from the same, or arteries other than adjacent ones, may join to form a small artery arcade. Assumption (3) excludes the possibility of arterioles emanating from any of the small vessels as a consequence of vessel dichotomous branching. Assumption (4) excludes the possibility of the arteriole linking up with another arteriole to form an arcade. Assumptions (2) through (4) mean that the contribution to vascular resistance of the small artery and arteriole anastamosing is not included in the topological model. The hemodynamic implications of these so called arcuate patterns are unknown. However, Nicoll and Webb (1956) have stated that the pattern serves a reservoir function in the sense that it helps to maintain a uniform arteriolar pressure distribution. This of course is speculation. However, if true it would be expected that their hemodynamic effects would be somewhat local, and their effect on calculations of resistance may be of second order importance. Similar speculation on the reservoir function of this type of arterial pattern has been put forward as concerns the pial arterial vessels on the cerebral cortex surface (Mechedlishvillie, 1969). It is the present author's feeling that the frequency with which these arcuate patterns appear in various vascular beds merits specific inquiry into their true hemodynamic or functional significance. However, to include such effects

at this time would require a large number of additional assumptions and exhaustive complexity for the topological model. Assumption (5) implies a single post capillary venule per capillary. In Wiedeman's original work all capillaries which took their origin from vessels other than arterioles were not counted as capillaries. The end of the capillary was defined as the point where an inflowing vessel joined it, the newly formed vessel being termed a post capillary venule. When the total number of vessels was tabulated, it was found that the number of post capillary venules exceeded the number of capillaries counted by a factor of approximately 3. During the present observations, it could be seen that some of the joining tributaries were capillaries which arose as side branches from vessels not in the field of the single branch artery being studied. Further, it was difficult to distinguish between the coalescing of two post capillary venules to form a third, thus increasing the post capillary venule count due to the arcuate patterns and continuously reversing flow pattern. Finally, if terminal arteriole is distinguished from arteriole as is here done, then a consistent characterization is the one given in figure 2.3. Assumption (6) does not appear to unduly restrict the generality of the analysis and is made to significantly simplify the representation.

B. Structure and Physical Properties

Structure refers to the composition of the vessel wall, the arrangement of the vessel wall constituents, and the mechanical

configuration of the vessel itself. Physical properties refer to the manifestation of the composite structural characteristics of the vessel when subjected to in vivo conditions. This would include the mechanical properties of the vessel, and its solute and fluid permeability when appropriate. There are three general ways in which these aspects interrelate with the other microvascular facets. The first is due to the functional relationship existing between vessel compliance and its physical properties. When the effect of the perivascular matrix is included, a quantitative relationship may be written which relates vessel compliance to the effective elastic moduli of the vessel wall and perivascular tissue and the lumen to wall thickness ratio (Noordergraaf, 1956). The second is due to the influence of structure and physical properties on the amount of control that can be affected by the vascular smooth muscle in the vessel wall. The third is due to the alteration in lumen diameter by pathological structural changes within the vessel wall or perivascular tissue.

Clearly, the details of such relationships depend on the particular vessel type, since, as we have pointed out, the structural and physical properties are not uniform. For our initial purposes, a detailed representation is not essential. The need to include compliance in the characterization is diminished because in the present analysis vascular bed resistance is determined on the basis of mean pressure and flow. The need to include the control facets of the vascular smooth muscle and lumen dependences on structural changes in the wall is not mandatory at this time because

the representation being in its "first generation" form represents the system to be controlled. However, as the model proceeds from its "first generation" form to an operational form these aspects will be incorporated (Ch. Four). Considerations of vessel compliance and the relationship between muscle contraction and vessel mechanical properties are thus dealt with in Chapter Four. In the present formulation, then, the specific assumption is that there is a distribution of vessel diameters, but the distribution is independent of changes in the mechanical properties of the vessels.

C. Hemodynamics (Fluid Dynamics and Fluid Properties)

1. General Approach

There are certain hemodynamic considerations which are unique to blood flow in the microvasculature. The general approach to evaluate flow produced by an imposed pressure gradient requires three general formative steps: (1) rheologic definition for the suspension; (2) fluid dynamic equations appropriate to the physical problem; and (3) inclusion of appropriate geometrical and boundary conditions.

The generalized fluid equations frequently employed as a starting point are the Navier-Stokes equations together with the equation of continuity. Use of the Navier-Stokes relationships assumes the applicability of the concepts of continuum and homogeneity. In the microcirculation the blood is not homogeneous in any classical sense. Further, the admissibility of the continuum approach to the entire suspension is not rigorous.

These difficulties notwithstanding, it is possible

to obtain approximations which are useful in characterizing microcirculatory hemodynamics by superimposing solutions obtained in regions in which the fluid dynamic equations are valid to an order sufficient for the purpose at hand. This superimposition process is itself subject to the requirement of linearity between the total set of describing equations within a specific region. What constitutes such a region, and hence the most appropriate mathematical approach consistent with present physiological knowledge, is to a large measure dictated by the characteristics of the fluid system associated with a particular region of the vasculature or vessel type.

In the microcirculation there are several "types" of vessels, and, as a consequence, there are several different formulations needed. For example, in the analysis of the capillary longitudinal pressure drop, an approach is to solve three fluid dynamic problems, one applicable to the plasma between cells, one applicable to the deforming red blood cell, and one applicable to the peripheral plasma layer between the red cell and vessel wall. The three solutions are then combined to characterize the total pressure drop. The equations are then solved simultaneously with the equations obtained for other vessel types both pre and post capillary to obtain a total solution. The approach adopted here is to use the individual solutions and characterize each vessel in terms of an equivalent resistance defined as the ratio of pressure gradient to volume flow. Each of the vessels illustrated in figure

2.3 is then represented by their appropriate resistance functions on the basis of branching distribution. Thus, each vessel is represented by as many axial sections as there are branches (see figure 2.6). Expressions are then derived for the input resistance at any level of the vasculature. In order to be able to analyze hemodynamic events within a specific vessel in greater detail, the equivalent source and drain resistances "seen" at any level are also determined. Separate analyses of the significance of well known rheologic factors (which include the viscosity dependence on hematocrit, the reduction in apparent viscosity with decreasing vessel lumen, and the concept of yield stress and its dependence on vessel erythrocyte concentration, in addition to the hemodynamics of the post capillary vasculature) have been carried out (Chapter Three). These factors are utilized for the calculations of bed input resistance for the topological model shown in figure 2.3. The significance of these factors is analyzed in Chapter Three, and appropriate aspects are included in the operational Microvascular Model which is developed in Chapter Four.

2. Mathematical Description

a. Pressure-Flow Relationships

In this section we are concerned with the mathematical description of the pressure-flow relationships in the several vessel types constituting the microvasculature. The principal objective is to obtain a resistance function expression for each vessel type.

i. Diameter of Vessel ≤ Undistorted Red Cell Dimension

The fluid dynamics of the arteriole, terminal arteriole, capillary and post capillary venule having a mean diameter range from 3.7 to 7μ are developed on the basis of single file erythrocyte flow. The resistance function is developed along the following lines. We consider n cells distributed in a vessel having total length l_T and inside diameter D_T. A portion of such a vessel is indicated in figure 2.4.

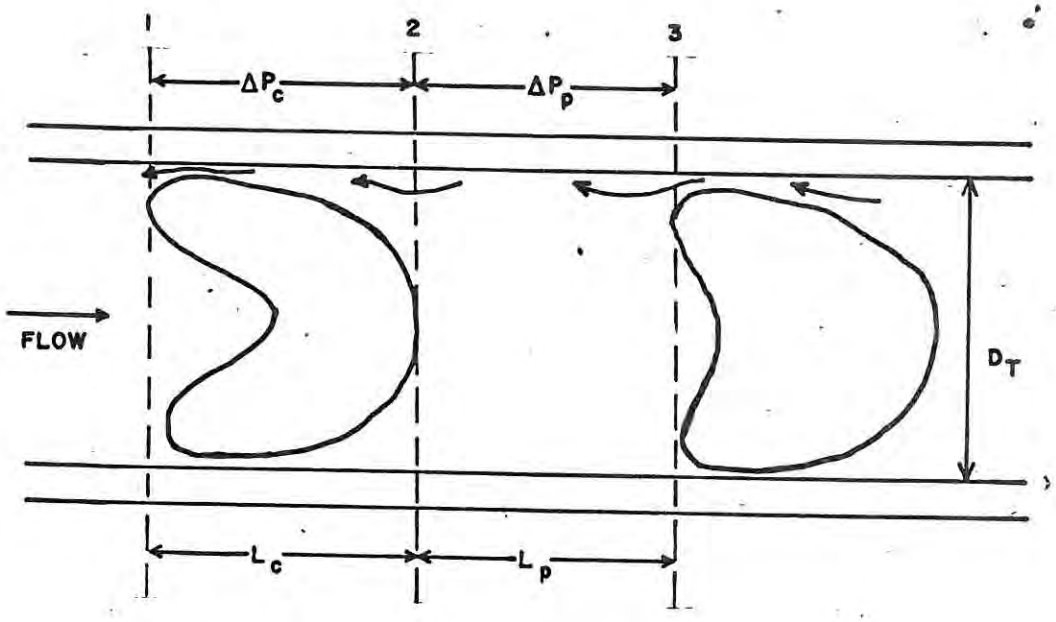

Figure 2.4. Representation of segment of microvessel in which vessel diameter is smaller than undistorted red cell dimension.

ΔP_c designates the pressure drop across the region occupied by one cell, and ΔP_p designates the pressure drop across the cell free region (plasma) between two adjacent cells.

The pressure drop in the plasma for a given mean flow deviates from that given by the Poiseuille relationship due to the flow field modification in the vicinity of the cells leading surface (surface 2) and due to the presence of the downstream cell and its alteration of the boundary conditions at surface 3. The influence of the upstream cell is approximated in the present analysis by utilizing and extending the results obtained by Barnard (1969), who treated the cell as a freely deformable surface and solved the resulting nonlinear boundary value problem numerically via successive iterations. By curve fitting we have represented the numerical solutions obtained for the three dimensional case in closed form, in terms of the ratio of undistorted cell dimension to inside vessel diameter.

Defining:

$\overline{\frac{\Delta P}{\Delta X_1}}$ = mean pressure gradient in the cell region;

η = plasma viscosity;

u_c = red cell velocity;

u_p = mean plasma velocity;

D_T = inside diameter of vessel;

D_c = undistorted cell dimension;

$\upsilon = D_c/D_T$;

k = a constant = 1.14.

The fundamental quantitative relationships for a single cell are the following:

$$(2.1)..... \frac{\overline{\Delta P}}{\Delta X_1} = \frac{16\eta u_c}{D_T^2}\left[1 + \left(\frac{\upsilon}{4}\right) + \left(\frac{\upsilon}{4}\right)^4\right]$$

$$(2.2)..... u_c = (2 - e^{-k/\upsilon})u_p$$

The effect of a finite separation of cells is approximated using the numerical solution due to Lee and Fung (1969), from which we develop a closed form characterization. Strictly speaking, effects within the plasma region for the idealized red cell shape analyzed by Lee and Fung depend on both cell separation and intravascular red cell dimension to vessel diameter. For a given cell separation and mean flow, the plasma region pressure gradient increases with increasing ratio of D_c/D_T. The maximum value of this ratio is unity and would constitute true plug flow. For this case, the mean pressure gradient in the plasma region may be expressed as:

$$(2.3)..... \frac{\overline{\Delta P}}{\Delta X_1} = \frac{32\eta u_p}{D_T^2}(1 + .6e^{-\beta s})$$

in which:

β_s = cell separation expressed in vessel diameters.

The total pressure drop across the length of the vessel is taken as the sum of the individual pressure drops. Using equations 2.1 and 2.2 together with the relationship:

$$(2.4)..... u_p = \frac{4Q}{\pi D_T^2}$$

which expresses the plasma velocity in terms of the flow, Q, we obtain:

$$(2.5)..... \frac{\overline{\Delta P}}{\Delta X_1} = \frac{64\eta Q}{\pi D_T^4} (2 - e^{-k/\upsilon})\left[1 + \left(\frac{\upsilon}{4}\right) + \left(\frac{\upsilon}{4}\right)^4\right]$$

Similarly from equation 2.3 we obtain:

$$(2.6)..... \frac{\overline{\Delta P}}{\Delta X_1} = \frac{128\eta Q}{\pi D_T^4} (1 + .6e^{-\beta s})$$

The pressure drop ΔP_{13} (figure 2.4) is:

$$(2.7)..... \Delta P_{13} = \Delta P_{12} + \Delta P_{23}$$

$$= \frac{128\eta Q}{\pi D_T^4}\left\{(2 - e^{-k/\upsilon})\left[1 + \left(\frac{\upsilon}{4}\right) + \left(\frac{\upsilon}{4}\right)^4\right]\frac{l_c}{2} + (1 + .6e^{-\beta s})l_p\right\}$$

The total average pressure drop across the entire vessel depends on the average number of cells, n, within the vessel and their distribution. For a given number of cells, the difference between the total pressure drop for a uniform distribution and a nonuniform distribution is small providing that a significant number of cells are not separated from each other by less than one half a vessel diameter. This follows from the calculation of the effective entry length (Fung, 1968). For the uniform case, the total pressure drop across the entire vessel is approximated as:

$$(2.8)..... \Delta P_T = n\Delta P_{13}$$

and the vessel resistance is given by:

$$(2.9)\ldots\ldots R = \frac{\Delta P_T}{Q} = \frac{128\eta}{\pi D_T^4} n\left\{(2 - e^{-k/\upsilon})\left[1 + \left(\frac{\upsilon}{4}\right) + \left(\frac{\upsilon}{4}\right)^4\right]\frac{l_c}{2} + (1 + .6e^{-\beta s})l_p\right\}$$

Equation 2.9 is the sought-after resistance function. The use of this equation in the model requires the appropriate values of n, l_p and l_c. These quantities are determined according to the following considerations.

For a given vessel average hematocrit, (H), total vessel volume V_T and red cell volume V_c, the number of cells n is:

$$(2.10)\ldots\ldots n = \frac{V_T H}{V_c} = \frac{\pi D_T^2 H l_T}{4V_c}$$

Using equation 2.10, together with the fact that the total vessel length is n times the sum of the plasma and cell gap for a uniform cell distribution, we may express the plasma region length as:

$$(2.11)\ldots\ldots l_p = \frac{4V_c}{\pi D_T^2 H} - l_c$$

Use of equation 2.11 requires knowledge of the average vessel hematocrit. It is convenient to express H in terms of the so-called feed or drain hematocrit H_s, since this is the quantity which is closer in magnitude to that which is measured by macroscopic blood sampling techniques. To accomplish this, we proceed by calculating the average concentration of cells exiting from the vessel in a time increment equal to that required for n cells to exit from the vessel. For an average cell velocity, u_c, and vessel length L_T,

this time increment is L_T/u_c. The volume exiting in this time is obtained from equation 2.4 as $\frac{\pi D_T^2}{4} \frac{u_p}{u_c} L_T$. The ratio of cell volume exiting to total volume exiting is the drain average hematocrit, which is equal to the average source hematocrit and is given by:

$$(2.12)..... \quad H_S = \frac{nV_c}{\frac{\pi D_T^2}{4} \frac{u_p}{u_c} L_T}$$

Using equation 2.12 together with 2.10 yields:

$$(2.13)..... \quad H = \frac{u_p}{u_c} H_S$$

Equation 2.13 allows the vessel hematocrit to be estimated in terms of the source hematocrit using equation 2.2.

It is also clear from equation 2.11 that for a given vessel the cell separation depends on the cell volume and cell intravascular length. The cell volume may be expressed in terms of the volume of an equivalent disk, or numerical values may be inserted on the assumption that the cell volume remains constant. However, the effective intravascular length, (l_c), depends upon the orientation and shape of the distorted red cell. From a pragmatic point of view, there are two modes of orientation, which need to be considered. One, illustrated in figure 2.4, is that of a cell orientation with the biconcave surface transverse to the flow. For this mode, the <u>in vivo</u> cell length is of the order of 4 microns. In the second mode, sometimes referred to as "edge on", the normally biconcave surface is parallel to the flow direction. For

this mode, the cell length is of the order of 8 microns. The actual orientation mode in vessels of the dimensions we are here considering is not yet fully clarified. The experimental model data of Sutera (1970) indicate the "edge on" configuration in these vessels, but even with this data, there is a considerable spread of the effective cell lengths for the same cell velocity ranging from 4.5 to 7.5 microns. Again according to Sutera's model and in vitro study of erythrocyte deformation, the cell distortion and length are functions of cell velocity, being less distorted and having smaller l_c at the lower velocities. Using Bernard's (1969) results on the shape of the distorted red cell, we calculate for an undistorted red cell diameter of 8 microns, an intravascular length of 3.4 and 3.1 microns corresponding to a 5 and 7.7 micron vessel respectively.

The calculation of the resistance of a particular vessel type is effected by choosing a value of l_c between 3 and 8 microns depending on the undistorted cell to vessel diameter. Using this value in equation 2.11 together with the value for the cell volume calculated for the deformed shape and the vessel hematocrit as determined by equation 2.13, the value of l_p is obtained. The value of β_s in equation 2.9 is determined based on this l_p and the vessel diameter. The value of υ is calculated for each of the vessels according to the experimentally obtained dimensional data. The value of n is determined using equation 2.10 with the average vessel lengths listed in table 2.1.

ii. Diameter of Vessel > Undistorted Cell Diameter

For those vessels which are very much larger than the red cell (i.e., main artery and artery), the pressure-flow relationship given by the Poiseuille equation is a reasonable approximation and is used in the present analysis. The general complicating factors which include the existence of the peripheral plasma layer, nonparabolic velocity profile and shear rate dependence of the effective viscosity, do not appear to significantly alter the resistance function provided that the appropriate value of viscosity is used in the Poiseuille equation.

The situation in the small artery and venule is more complicated in that the flow region lies between the single cell capillary case and the "continuum" main artery case. In the venous vessels, there is the further complication associated with the existence of an effective yield stress, which becomes increasingly important as the shear rate becomes lower. We have examined the significance of these factors (see Chapter Three), and our preliminary findings indicate that with respect to the calculation of bed input resistance, the direct effect of these factors may be neglected in the normal state. The principal reason is that the velocity gradients in the arterial vessels are sufficiently large to make these factors of second order importance with respect to the shear flow pressure drop. We have thus represented the flow regime and more specifically the resistance functions of these vessels in a fashion similar to the larger vessels (Noordergraaf, 1969).

b. Vessel Representation and Vascular Resistance Distribution

In this section we are concerned with the problem of representing the vessels and the interrelationships of vessels in such a way that will permit calculation of the resistance at any level of the microvasculature in terms of the resistance functions of the several vessel types and the vessel distributions.

i. Input Resistance

The procedure to determine the bed input resistance and resistance distribution is as follows. Each vessel of the topological model of figure 2.3 is represented as a cascade of symmetrical "T" sections of the form shown in figure 2.5. The characteristics of the section may be expressed in terms of four parameters known as the A, B, C, and D parameters defined by the equations shown in figure 2.5. The number of cascaded sections used for each vessel type is equal to the average number of branches of that vessel. For example, the first order vessel of figure 2.3, which has on the average 12 branches, is represented by 12 symmetrical sections. This applies to all such first order vessels (13 in all). The other order vessels are similarly represented. The longitudinal impedance Z_1 is the same throughout the vessel axial length. A typical vessel representation would thus appear as shown in figure 2.6. For a given vessel order, Z_1 is determined by the method described in section a. The quantity Z_2 represents the impedance seen looking toward the capillary. Thus Z_2 is in effect

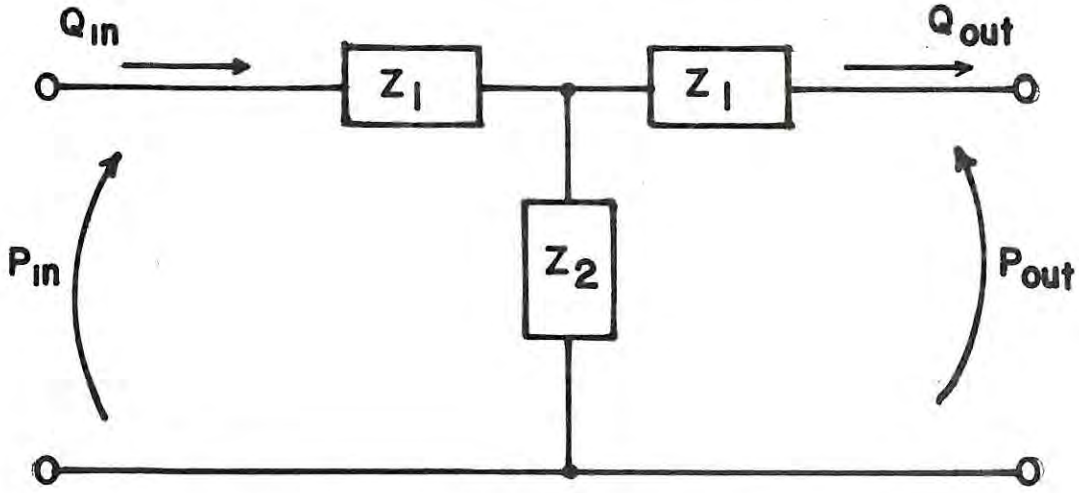

$$P_{in} = A\,P_{out} + B\,Q_{out}$$

$$Q_{in} = C\,P_{out} + D\,Q_{out}$$

Figure 2.5. Sym. "T" network used to represent segments of vessels. A, B, C, and D are network parameters which depend on Z_1 and Z_2. These parameters characterize the relationship between input pressure (P_{in}), output pressure (P_{out}), input flow (Q_{in}) and output flow (Q_{out}). Z_1 is half the longitudinal impedance of a vessel segment between two adjacent branches. Z_2 is the impedance of the remainder of the vascular circuit as seen at the branch junction.

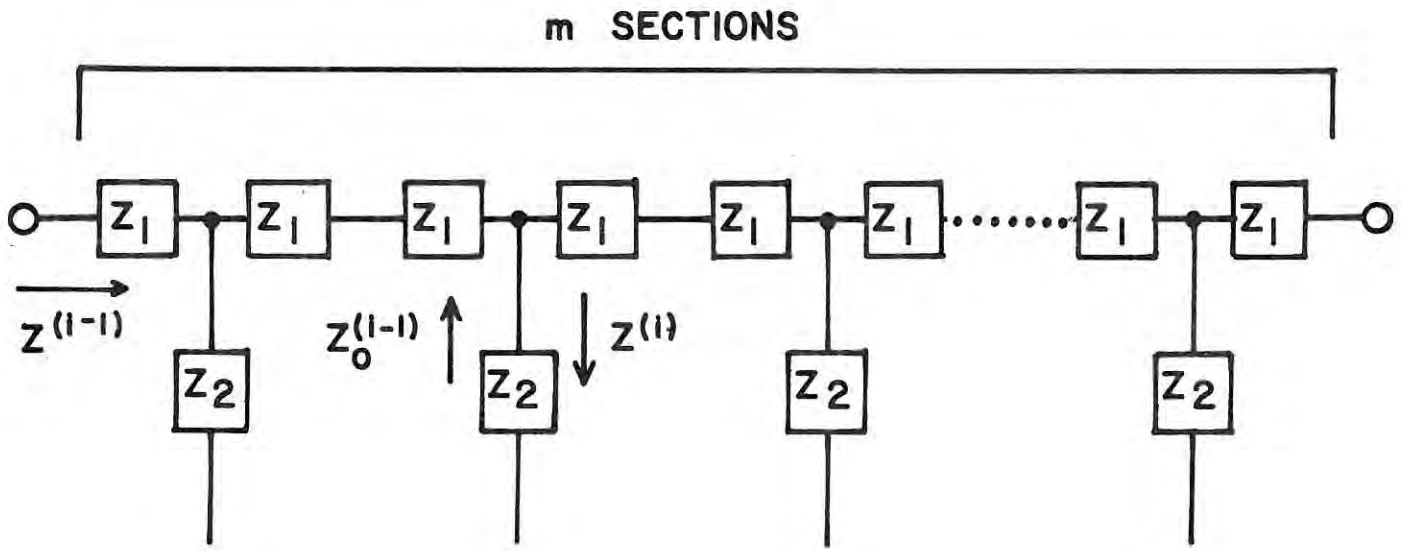

Fig. 2.6. Representation of vessel by cascaded sections. Cascading m vessel segments of the type shown in figure 2.6 (m = number of branches) results in the general representation shown. $Z^{(i)}$ represents the total impedance seen looking toward the capillary at a particular branch site. For i = 2 this would correspond to the input impedance looking into the second order branch (small artery of figure 2.3), for i = 3, $Z^{(i)}$ corresponds to the third order branch input impedance (arteriole in figure 2.3), and so on. Each value of $Z^{(i)}$ serves as the Z_2 value for the computation of input impedance of the i - 1 order vessel, $Z^{(i-1)}$. The quantity $Z_0^{(i-1)}$ represents the impedance seen looking from any branch back towards its parent vessel with all other vascular curcuits intact. $Z_0^{(i-1)}$ thus represents the driving source impedance as seen by the i^{th} order branching level.

the input impedance of the remainder of the vascular circuit and depends on its impedance distribution. This input impedance is denoted as $Z^{(i)}$. For i = 1, this would correspond to the input impedance looking into the first order vessel at a particular branch site, for i = 2, the second order vessel, and so on. Each value of $Z^{(i)}$ serves as the Z_2 value for the computation of the $Z^{(i-1)}$ input impedance. Applying the results of Bartlett (1935), the input impedance, $R^{(i)}$, at any level may be shown to be a special case of the following general impedance function.

$$(2.14)\ldots\ldots\ Z^{(i)} = \frac{Z_L(d_1 - d_2F^m) + d_1d_2(F^m - 1)}{Z_L(1 - F^m) + (d_1F^m - d_2)}$$

in which:

$$d_1 = \frac{A - D}{2C} + \sqrt{\left(\frac{A - D}{2C}\right)^2 + \frac{B}{C}}\ ;$$

$$d_2 = \frac{A - D}{2C} - \sqrt{\left(\frac{A - D}{2C}\right)^2 + \frac{B}{C}}\ ;$$

A,B,C,D = elements of [a] matrix representing a section of the i^{th} order vessel;

m = the number of sections representing the i^{th} order vessel = number of branches of i + 1 order;

Z_L = the effective terminating impedance of the m^{th} segment;

$$F = \frac{A - Cd_1}{A - Cd_2}\ .$$

Successive applications of equation 2.14 are used to calculate the input resistance at each vascular level.

ii. Output Resistance

By output resistance is meant the equivalent source resistance through which pressure and flow are

coupled to a vessel of order i. This resistance is denoted as $R_0^{(i)}$. For example, the resistance seen by an arteriole is $R_0^{(3)}$, which would correspond to $R_0^{(SA)}$ shown in figure 2.3. Since there are m_i vessels of order i for each vessel of order (i - 1), it is convenient to determine $R_0^{(i)}$ for a representative vessel. In the present analysis, we choose the vessel representing the $m_i/2$ branch. Successive applications of equations 2.14 allow $R_0^{(i)}$ to be determined when applied to the topology shown in figure 2.3.

III. Results and Comparison with Experimental Data

A. Resistance Distribution Determined from Topological Model

Table 2.2 summarizes the results obtained for the calculation of input and output resistances at different vascular levels using the formulations and methods described in section II. Note that both the input and output resistances, i.e., the equivalent driving point impedance for a given vessel type, increase as the capillary is approached from the arterial side.

Table 2.2. Input, R_i, and output, R_0, resistance at different orders of branching. Superscripted numbers denote branching order for which resistance is determined. Branching orders 1, 2, 3 and 4 correspond to artery, small artery, arteriole and terminal arteriole as shown in figure 2.3.

	dynes cm^{-5} sec.
$R_i^{(1)}$	3.49×10^9
$R_i^{(2)}$	5.9×10^9
$R_i^{(3)}$	5.2×10^{10}
$R_i^{(4)}$	3.8×10^{11}
$R_0^{(4)}$	1.8×10^{11}
$R_0^{(3)}$	2.9×10^{10}
$R_0^{(2)}$	9.2×10^9
$R_0^{(1)}$	2.1×10^9

B. Experimental Data

In order to evaluate the accuracy of the model predictions, an experimental protocol was carried out with the principal objective of measuring the input resistance at the artery level [$R_i^{(1)}$].

1. Method

Figure 2.7 is a diagrammatic representation of the experimental method. A micropipette is inserted into the main artery entering the wing in a retrograde fashion. The micropipette is connected to a small syringe filled with buffered saline and through a "T" connector to a pressure transducer. The microscopic image of an artery (branch of main artery) is projected via a closed circuit TV system onto the monitor. Two photo conductors, suitably calibrated, are positioned on the monitor along the artery, and separated by a known axial distance. The red cell concentration in the artery is momentarily decreased by forcing the red cell column in the main artery to the proximal side of the artery branch point by a slight increase in syringe applied pressure. The pressure is then returned to its initial value, and the normal type flow is returned to the artery. The photo cells measure the transit time of both the initial decrease in opacity and subsequent increase in opacity (bolus). The time delay between a known photo cell separation allows for the calculation of the mean velocity, which is then used to calculate the flow, since the diameter of the vessel is known. The ratio of the pressure measured using the low compliance Micro-Dot transducer at the branch entrance site to the flow determined in this fashion is the resistance, $[R_i^{(1)}]$.

In addition to these direct measurements, use was made of data obtained by Wells (1971) using rubidium tagging in which total wing flow was measured to be [.0012 $cm^3 sec^{-1}/gm$]. Based on

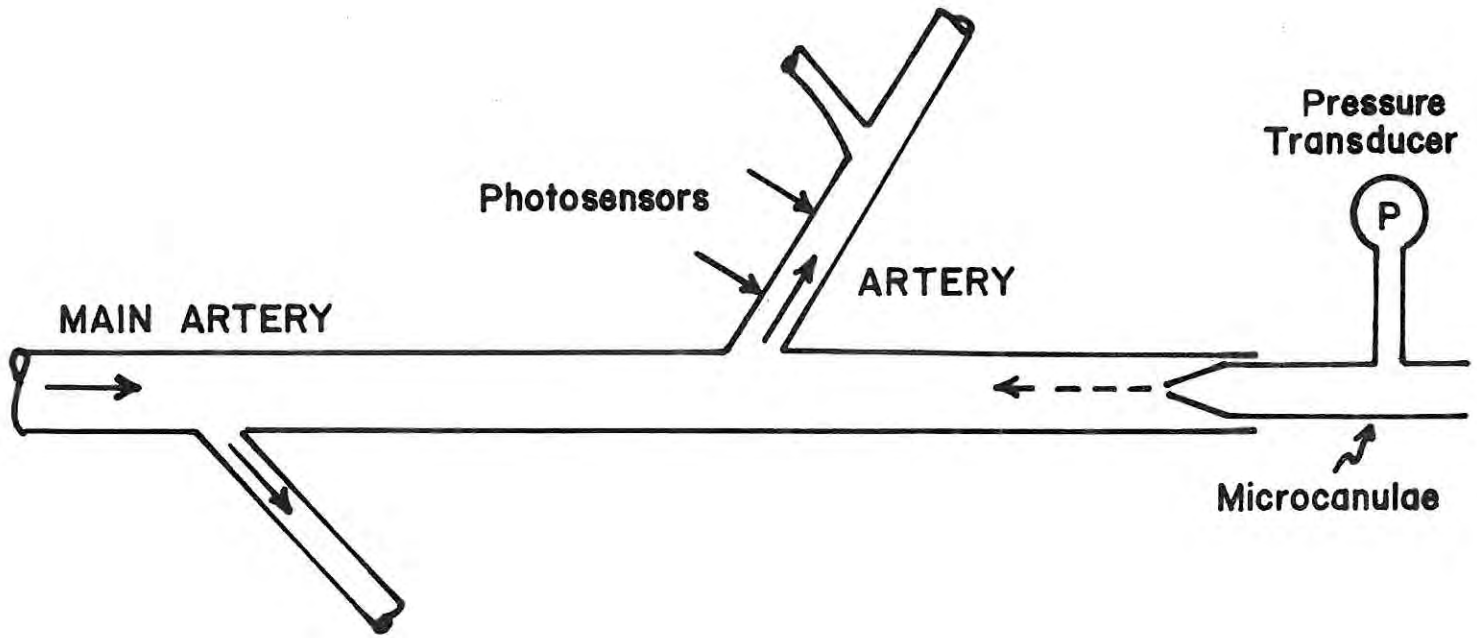

Figure 2.7. Diagrammatic representation of experimental setup to measure pressure and flow. See text for description.

12 vascular units supplied by the main artery and a wing weight of .3 gms, this means a flow per vascular unit of 2.9×10^{-5} cm^3/sec.

2. Comparison of Model and Experimental Results

Table 2.3 below summarizes the results for the three methods of determining $R_i^{(1)}$, i.e., as calculated from the model and the two experimental approaches. The close agreement between the model prediction and the experimentally determined values may be viewed as an encouraging result. It tentatively reflects an affirmative answer to the question whether the characterization of the vasculature used can be relied upon to adequately predict vascular bed resistance in a normal preparation. Measurement of resistances at other levels was precluded due to the lack of appropriate pressure measuring system.

Table 2.3. Comparison of calculated and derived values of $R_i^{(1)}$.

	dynes cm^{-5} sec.
$R_i^{(1)}$ calculated from model	3.49×10^9
$R_i^{(1)}$ derived from experimental data	3.6×10^9
$R_i^{(1)}$ calculated from experimental data of Wells (1971)	3.45×10^9

inducing treatment. The hypertension determined by measurement of pressure in the tail artery showed the existence of two groups classified as low, or intermediate hypertensive (H_L), and high hypertensive (H_H). The data are presented in Table 2.4 (Asterisked quantities were calculated by us). The question that was posed was the following one: Will the model predict the measured changes in blood pressure when the morphological changes in the hypertensive animal are appropriately incorporated?

A. Method

The method employed is to first use Freedman's data to calculate the percentage change in vascular dimensions in artery and arteriole. Then characterize the difference in vessel lumen between experimental controls (c) and the two hypertensive subgroups by a radius reduction factor J. Similarly calculate pressure increase factors denoted as S for systolic and D for diastolic. Mean pressure is calculated as diastolic plus one-third of the pulse pressure. Then use the topological model as a reference vascular bed and its input resistance as a reference resistance, program the vascular model dimensions in accordance with the calculated radius reduction factors. Calculate the input resistance of the altered vascular model, and form the ratio of this value with that obtained for the model with control vascular dimensions. Denote this ratio as R_{LC}, R_{HC}, or R_{LH}, depending on whether the comparison is between subgroups H_L and C, H_H and C, or H_H and H_L, respectively. Call these ratios resistance increase factors. Finally, compare the calculated resistance increase factors as determined from the model

Table 2.4. Data for arterial vessel changes accompanying deoxycorticosterone acetate induced hypertension. a is vessel radius in microns; h is vessel wall thickness in microns. Ps, Pd and $\overline{P}$ correspond to systolic, diastolic and mean pressures, respectively, expressed in mmHg. Quantities with asterisks are calculated by this author; otherwise, data are due to Freedman (1971). $\overline{P}$ is calculated as $Pd + \frac{1}{3}(Ps - Pd)$.

Superficial Epigastric Artery (values are means)

	a	h	a/h*	Ps	Pd	$\overline{P}$*
Control	144	30	4.8	138	73	95
H_L	124	35	3.5	156	82	107
H_A	106	36	3.0	194	113	140

Arteriole

	a	h*	(a/h)*	Ps	Pd	$\overline{P}$*
Control	33	3.4	9.8	138	73	95
H_L	30	3.9	7.7	156	82	107
H_A	27	4.3	6.3	194	113	140

with the pressure increase factors as calculated from the data.

B. Results

Table 2.5 is a tabulation of the calculated radius decrease and pressure increase factors. Table 2.6 is a tabulation of the hypertensive input resistances, $[R_H^{(0)}]$, resistance increase factor and mean pressure increase factor corresponding to two separate comparisons. In the first column of table 2.6, the model, with characteristics given by table 2.1, is used to represent the vascular state of the experimental control group, and the increase in resistance for the low hypertensive group is presented in terms of the resistance factor. The resistance factor predicts an increase in mean pressure by a factor of 1.32. The measured increase is only 1.13. In the second column, the vascular model is used to represent the vascular state of the low hypertensive group, and the increase in resistance of the high hypertensive group is expressed as the resistance factor. The agreement between the model prediction with respect to the mean pressure in the high hypertensive group in this case is better (1.44 vs. 1.31). In each case the model predicts a higher mean pressure than was actually measured.

Table 2.5. Radius and pressure factors calculated from data of Freedman (1971). J_{CL} is the ratio of low hypertensive radius to control radius. J_{CH} is the ratio of high hypertensive radius to control radius. J_{LH} is the ratio of high hypertensive radius to low hypertensive radius. S_{CL} is the ratio of low hypertensive systolic pressure to control pressure. S_{CH} is the ratio of high hypertensive systolic pressure to control pressure. S_{LH} is the ratio of high hypertensive systolic pressure to low hypertensive systolic pressure. D_{CL}, D_{CH}, and D_{LH} are similar ratios for diastolic pressures. Flow is assumed constant.

	Radius Factors			Pressure Factors					
	J_{CL}	J_{CH}	J_{LH}	S_{CL}	S_{CH}	S_{LH}	D_{CL}	D_{CH}	D_{LH}
Artery	.86	.74	.86	1.13	1.39	1.24	1.12	1.60	1.38
Arteriole	.91	.82	.90	1.13	1.39	1.24	1.12	1.60	1.38

Table 2.6. Results of model calculation using radius factors of table 2.5. $R^{(0)}_{reference}$ is the input resistance as calculated from the topological model. $R^{(0)}_{H}$ is the input resistance calculated from the topological model with vessel diameter changes simulating those observed by Freedman. Resistance factor is the ratio $R^{(0)}_{H}/R^{(0)}_{reference}$. Mean pressure factor is the calculated ratio of hypertensive mean pressure to control mean pressure. Resistances are in units of 10^8 dynes cm^{-5} sec.

	Control Group compared with Group L	Group L compared with Group H
$R^{(0)}_{reference}$	4.82	4.82
$R^{(0)}_{H}$	6.96	6.96
Resistance factor	1.44	1.44
Mean pressure factor (measured by Freedman)	1.13	1.31

V. Discussion

In this chapter a first generation model of the vasculature of the bat wing has been developed. It has been shown that given sufficient information about the architecture and topology it is feasible to develop a microvascular representation using theoretical fluid dynamic formulations. The specific aspect with which the bulk of this chapter was concerned was the prediction of the vascular bed resistance. This the model did quite well. The model predictions were within 4% of the measured values obtained by the author, and as calculated from data available in the literature. From several points of view the model is not excessively complex. It does not deal in impedance, but rather resistance. A number of the complicating rheologic factors are not yet included. The post capillary vasculature is not yet included in any extensive fashion. Yet the results of the model prediction were as close to the measured values as one would have dared to hope for. Could it be that the topology, which was dealt with extensively, together with appropriate formulations of the hemodynamics, are the principal determinants of vascular bed resistance? And that other factors in the normal state play a small role? The results obtained here would support such a notion but hardly prove it. With the available instrumentation it was possible to measure the resistance at only one level of the vasculature. Thus we can not yet make any statements about the effect of these "other factors" on events within the microvasculature. Another aspect of interest in this chapter

was the degree to which the wing vasculature could be used as a "model" vasculature representing whole body vascular changes. Thus the model was evaluated as a hypertensive pressure predictor when subject to morphological changes in the vessels.

Perfect agreement between the predicted and measured pressure rise corresponding to the two hypertensive subgroups would mean 1) that the vessel dimensional changes measured on a sample basis are characteristic of all vessel changes; 2) that the model topology and structure adequately represent the essential characteristics of the entire vascular system with respect to bed resistance, and 3) other changes in vascular or hemodynamic characteristics are negligible with respect to their effect on bed resistance. That the perfect agreement is not achieved is not surprising in view of the several difficulties in interpretation of the present results. The measured data distinguish between two vessel types, whereas the vascular model consists of five vessel orders on the arterial side. Thus, it is necessary to assign the radius reduction factors according to some criteria developed for the purpose. In the results that are presented here, the main artery radius changes were programmed to correspond to the epigastric artery changes and the other vessel orders to the arteriole hypertensive changes. Assuming that this is an adequate description of changes within the vascular region measured, there is no direct evidence that these changes are representative of changes within the remaining vascular beds. If we assume that they are representative, then the differences in the

relative contribution to total resistance of each bed must be considered. In the present analysis, the predicted pressure increase is based on a uniform contribution and is probably a major reason why the pressure increase is larger than that measured. Another factor is the effect of possible changes in cardiac output on the measured pressure. Cardiac output was not measured, but small reductions in the hypertensive groups would have the tendency to bring the predicted values closer to the measured values of pressure. The fact that the predictive quality of the model was best when the comparison was made between the low and the high hypertensive group could indicate that there were differences other than dimensional between the control and hypertensive groups, but that because these were differences common to both hypertensive groups, they were less significant with respect to the pressure comparison.

The inadequacy of the hypertension prediction notwithstanding, the microvascular representation developed and utilized represents an initial and basic framework for microvascular characterization. As it is presently formulated, it is strictly applicable to the bat wing. Its significance is that it represents a characterization method applicable to other vascular beds providing that appropriate specific refinements associated with other beds are incorporated. The major advantage of the representation used is that the effects of changes in dimensions of individual vessel orders as they relate to changes in vascular bed resistance may be incorporated and evaluated. Thus it provides the required framework for

incorporating nonuniform systems and local control acting on the several vessel orders and evaluating the composite and separate significances of these controls on changing vascular resistance. This control represents a parametric change of the dimensional and physical properties of identifiable vessels which in turn alter vascular bed resistance and microvascular resistance distribution. Such controls have not been implicitly incorporated here, because it was our purpose to develop a first generation model of the system to be controlled and because of the lack of quantitative information concerning the characteristics of this parametric control. However, by utilizing the basic representative approach developed here, a foundation for a more comprehensive microvascular characterization of specific vascular regions of the body is now available and will be utilized in Chapter Four. Further, by modifying the basic vessel segment representation to include frequency dependent parameters, it is possible to use the topological model structure to determine the input impedance at the several branching order levels as a function of frequency, i.e., $Z_{in}(\omega)$.